Digital measuring scheme for half-wave voltage of Y-tap multiple integrated optical circuit

Yuanhong Yang (杨远洪) and Hongtao Yu (于洪涛)

The Institute of Optoelectronics Technology, Beijing University of Aeronautics & Astronautics, Beijing 100083

Received June 18, 2004

A high-precision digital measuring scheme for half-wave voltage of Y-tap multiple integrated optical circuits is proposed. This scheme is based on Sagnac interferometer modulated with digital step waveform whose frequency is half of eigen frequency of the interferometer. The technology and measuring precision are discussed. An experimental setup is made and the temperature-dependences of half-wave voltage of two samples are studied. Analysis and experimental study prove that this scheme is convenient and accurate.

OCIS codes: 130.3120, 120.5790, 060.5060.

Y-tap multiple integrated optical circuit (MIOC), which has single polarization waveguide Y-tap fabricated in $LiNbO_3$ with annealing proton exchanged (APE) technology and two phase modulators based on Pockels effect, is one of the key components of close-loop fiber optic gyroscope (FOG). It takes the roles of mode filter (polarizer), directional coupler, and phase modulator in FOG[1]. As an electro-optic component, the half-wave voltage V_π, which is defined as the voltage that can produce π phase change of light wave propagating in MIOC, is a special parameter that will vary with environmental temperature and directly bring nonlinearity in close-loop FOG. Model compensation is an effective approach to reduce this defect[2], so it is very important to get accurate model with precision measuring. In general, Mach-Zehnder interferometer formed with two MIOCs can be used to measure V_π and moderate precision can be gotten with complex system and special modulation technology[3]. However, the measuring precision is limited because this system has poor stability. To satisfy the demand of high precision measuring and modeling, an all-digital scheme based on Sagnac interferometer is proposed and discussed. With this technology, two MIOC samples are studied.

Figure 1 is the schematic diagram for V_π measurement. The superluminescent diode (SLD), coupler, detector, fiber coil, and the MIOC to be measured compose a Sagnac interferometer. In Fig. 1, the coupler takes the charge of sending the light from SLD to MIOC and guiding the coming back signal to the detector; MIOC and fiber coil form a closed optical path, the light from point J is splitted into two parts propagating along converse direction and then recombining at J. The interference output signal is monitored by a digital oscillograph, it

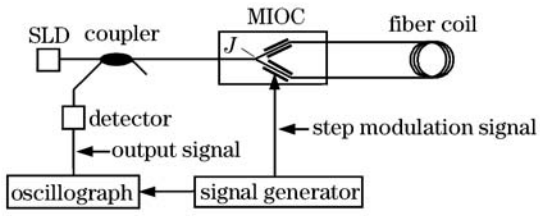

Fig. 1. Schematic diagram for V_π measurement.

can be described as[1]

$$v_o = K(1 + \cos\phi), \tag{1}$$

where K is the coefficient related with the incident optical power on detector and the gain of detector module, ϕ is the nonreciprocal phase which can be produced by rotation or nonreciprocal modulation.

Herein, the measuring system is always still and ϕ is attributed to nonreciprocal modulation only. Figure 2 shows the modulation signal and relative waveforms when a digital step modulation signal generated by a digital signal generator is added to the electrode of MIOC. In this figure, waveform A represents the relation of v_o and ϕ described by Eq. (1). The step height and width of modulation signal C are V_s and τ (τ is the time needed for light transmitting through the fiber coil once), respectively, and the frequency is half of the eigen frequency of the Sagnac interferometer, the period of modulation signal is 4τ. Because the modulator is at one end of the coil, the clockwise (cw) and counter clockwise (ccw) light signals are modulated at different time. The time difference is τ which is attributed to the fiber coil delay. The phase produced by the modulator can be calculated by[1]

$$\phi(t) = \phi_m(t) - \phi_m(t - \tau), \tag{2}$$

where $\phi_m(t)$ and $\phi_m(t - \tau)$ represent the modulation

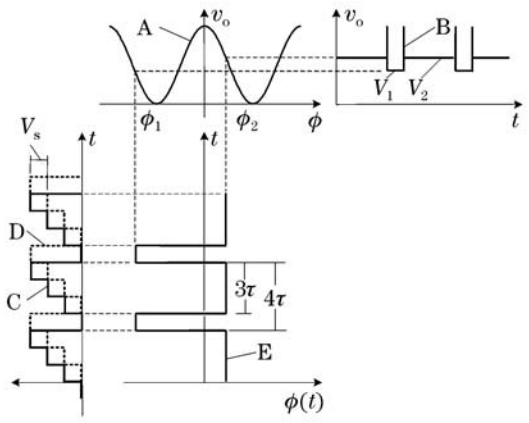

Fig. 2. Digital step modulation signal and relative waveforms.

phases of ccw and cw propagating light, namely waveform C (solid lines) and D (dashed lines) in Fig. 2. Waveform E in Fig. 2 represents $\phi(t)$ which is described by Eq. (2) and has the period of 4τ. Waveform B is the output of detector. During a modulation period, the modulation phase differences ϕ_1 and ϕ_2 for ccw and cw light will be

$$\phi_1 = \phi(t) = -\frac{3\pi V_s}{V_\pi}, \quad (0 < t < \tau), \tag{3}$$

$$\phi_2 = \phi(t) = \frac{\pi V_s}{V_\pi}, \quad (\tau < t < 4\tau), \tag{4}$$

the corresponding outputs are

$$V_1 = K[1 + \cos(\phi_1)], \tag{5}$$

$$V_2 = K[1 + \cos(\phi_2)]. \tag{6}$$

Let $V_1 = V_2$, combining Eqs. (3)−(6), the first non-zero solution of V_π is

$$V_\pi = 2 \cdot V_s. \tag{7}$$

V_s is artificially set, so adjusting V_s from low to high, when V_1 is equal to V_2 for the first time, the half-wave voltage V_π is $2V_s$ and the accurate measurement is realized. The practical waveforms during measuring procedure are shown in Fig. 3. The difference between V_1 and V_2 varies obviously when V_s changes 2 mV.

When $V_1 \approx V_2$, $\phi_1 \approx -3\pi/2$, and $\phi_2 \approx \pi/2$, V_1, V_2 are very sensitive with the variation of V_s, as shown in Fig. 3. Let

$$\Delta V = V_2 - V_1, \tag{8}$$

ΔV can be used to judge whether Eq. (7) is satisfied. From Eqs. (3)−(6), Eq. (8) can be

$$\Delta V \approx 2K \sin\left(\frac{2\pi \cdot \Delta V_s}{V_\pi}\right). \tag{9}$$

The value of ΔV_s is determined by the resolution of signal detection system. This measuring technology is similar to the signal processing in close-loop FOG. We can use it to estimate the accuracy of ΔV_s. For example, 1°/hour bias drift can be achieved easily in FOG and it approximately corresponds to 10^{-6}-rad phase drift. In Eq. (9), this means $2\pi \cdot \Delta V_s / V_\pi \approx 10^{-6}$. V_π is only a few voltages, ΔV_s will be much smaller. This proves that this scheme can achieve very high accuracy. Otherwise, when $V_1 = V_2$, Eq. (7) is satisfied and $\phi_1 = -3\pi/2$, $\phi_2 = \pi/2$, the measuring veracity is guaranteed naturally.

From Eqs. (3)−(6) and (8), we know it is the 2π phase difference between ϕ_1 and ϕ_2 that makes Eq. (7) satisfied. During a modulation period, which is about a few microseconds, we can define whether $V_1 = V_2$ is satisfied and the measuring procedure can be thought as instantaneous. So, any nonreciprocal phase shift induced by other factors, such as environmental temperature varying, rotation, etc., will not affect the measurement because these changes are all slow. With the same reason, the measurement is insensitive to the small variation of K induced by optical path loss change or source power change in Eq. (1). This means the measurement is insensitive to environment and high precision can be achieved.

A digital auto measuring setup is made based on Fig. 1 and shown in Fig. 4. The output from detector is digitized with a 12-bit analogy/digital converter (A/D), the digital step signal is generated with a 12-bit digital/analogy converter (D/A) and the computer takes the role to calculate the voltage difference and adjust the step height. The length of fiber coil is about 500 m and the operation wavelength is 1.3 μm. In the experiment, only the MIOC which is connected with coupler and fiber coil by fuse splicing is mounted in a temperature chamber (TC), V_π is measured at different temperature from −40 to 60 °C.

Two MIOC samples from different companies have been tested. The results are shown in Figs. 5 and 6. The V_π variations are respectively 0.163 and 0.251 V within

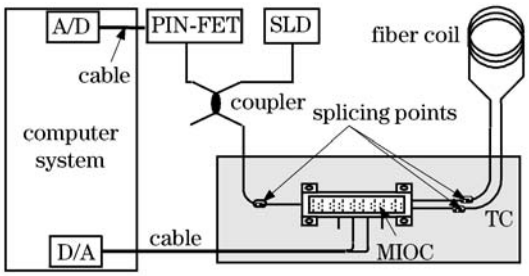

Fig. 4. Digital experimental setup. FET: field effect transistor.

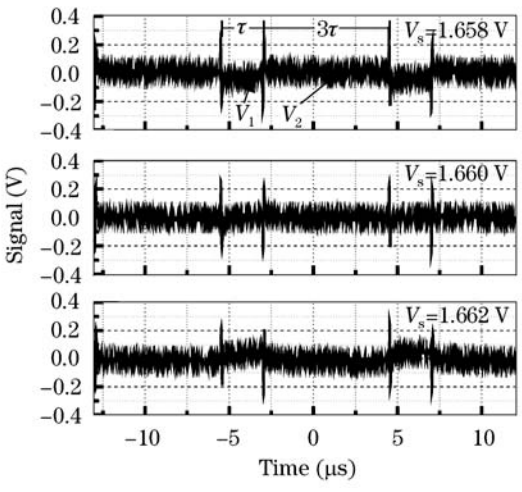

Fig. 3. Waveforms during the measuring procedure.

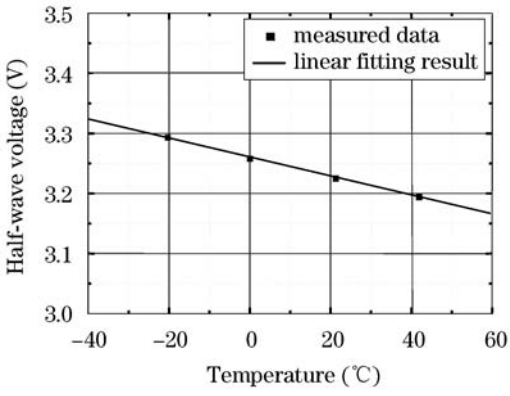

Fig. 5. Test result of sample 1.

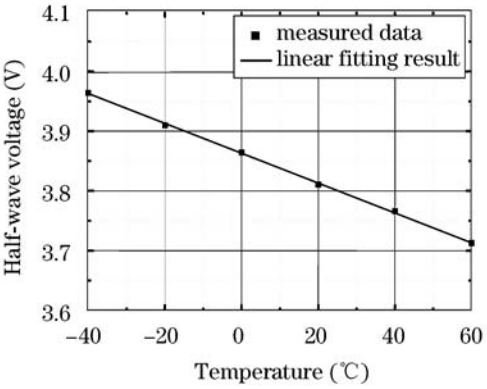

Fig. 6. Test result of sample 2.

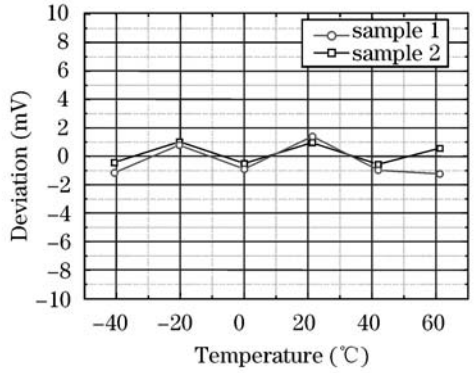

Fig. 7. Linear deviation of the tested data.

the whole temperature range from −40 to 60 °C. After least square polynomial fit with the measured data from −40 to 60 °C, the variations are found to be linear in the test temperature range and the temperature coefficients are 503 and 654 ppm/°C, respectively. The result is similar as the data reported in Ref. [4]. The absolute linear deviation is calculated and the value is about 1 mV (see Fig. 7). This proves that the measurement has high precision and the temperature dependence of V_π has good linearity.

In summary, experimental study and detail discussion demonstrate that the proposed scheme can measure V_π of Y-tap MIOC conveniently and accurately. Experimental study on the temperature-dependence of V_π of MIOC also shows that V_π decreases as temperature increases with good linearity. With this digital scheme, the accurate temperature model can be obtained easily.

This work was supported by the National Natural Science Foundation of China under Grant No. 60207002. Y. Yang's e-mail address is yhyang@263.net.cn.

References

1. H. Lefevre, *The Fiber-Optic Gyroscope* (Artech House, Boston, London, 1993) pp. 276—284, p. 32, p. 33.
2. R. Mauricio, G. Spahlinger, and M. Kemmler, Proc. SPIE **2837,** 199 (1996).
3. Y. H. Yang, J. Ma, and W. X. Zhang, Chin. J. Lasers B **3,** 538 (1994).
4. G. A. Pavlath, Proc. SPIE **2837,** 46 (1996).